JOURNAL OF ENVIRONMENTAL SCIENCES 99 (2021) 80–89

Available online at www.sciencedirect.com

ScienceDirect

www.elsevier.com/locate/jes

JES JOURNAL OF ENVIRONMENTAL SCIENCES

www.jesc.ac.cn

Diverse molecular compositions of dissolved organic matter derived from different composts using ESI FT-ICR MS

Minru Liu[1,2], *Yunkai Tan*[1,2], *Kejing Fang*[1,2], *Changya Chen*[3,*], *Zhihua Tang*[1,2,*], *Xiaoming Liu*[4], *Zhen Yu*[4]

[1] *Guangdong Provincial Key Laboratory of New and Renewable Energy Research and Development, Guangzhou Institute of Energy Conversion, Chinese Academy of Sciences, Guangzhou 510640, China*

[2] *CAS Key Laboratory of Renewable Energy, Guangzhou Institute of Energy Conversion, Chinese Academy of Sciences, Guangzhou 510640, China*

[3] *Hunan Provincial Key Laboratory of Fine Ceramics and Powder Materials, School of Materials and Environmental Engineering, Hunan University of Humanities, Science and Technology, Loudi, 417000, China*

[4] *Guangdong Key Laboratory of Integrated Agro-environmental Pollution Control and Management, Guangdong Institute of Eco-environmental Science & Technology, Guangzhou 510650, China*

ARTICLE INFO

Article history:
Received 9 March 2020
Revised 30 May 2020
Accepted 10 June 2020
Available online 29 June 2020

Keywords:
Molecular characterization
Dissolved organic matter
Compost
ESI FT-ICR MS

ABSTRACT

Dissolved organic matter (DOM) derived from various composts can promote significant changes of soil properties. However, little is known about the DOM compositions and their similarities and differences at the molecular level. In this study, the molecular compositions of DOM derived from kitchen waste compost (KWC), green waste compost (GWC), manure waste compost (MWC), and sewage sludge compost (SSC) were characterized by electrospray ionization coupled with Fourier transform ion cyclotron resonance mass spectrometry (ESI FT-ICR MS). The molecular formulas were classified into four subcategories: CHO, CHON, CHOS, and CHONS. The KWC, MWC, and SSC DOM represented the highest fraction (35.8%-47.4%) of CHON subcategory, while the GWC DOM represented the highest fraction (68.4%) of CHO subcategory. The GWC DOM was recognized as the nitrogen- and sulfur-deficient compounds that were less saturated, more aromatic, and more oxidized compared with other samples. Further analysis of the oxygen, nitrogen-containing (N-containing), and sulfur-containing (S-containing) functional groups in the four subcategories revealed higher organic molecular complexity. Comparison of the similarities and differences of the four samples revealed 22.8% ubiquitous formulas and 17.4%, 11.1%, 10.7%, and 6.3% unique formulas of GWC, KWC, SSC, and MWC DOM, respectively, suggesting a large proportion of ubiquitous DOM as well as unique, source-specific molecular signatures. The findings presented herein provide new insight into the molecular characterization of DOM derived from various composts and demonstrated the potential role of these different compounds for agricultural utilization.

* Corresponding authors.
E-mails: liumr@ms.giec.ac.cn (M. Liu), yuer-17@163.com (C. Chen), tangzh@ms.giec.ac.cn (Z. Tang).

https://doi.org/10.1016/j.jes.2020.06.011
1001-0742/

Introduction

Kitchen waste, green waste, manure waste, and sewage sludge are the typical organic solid wastes in China (Liu et al., 2017; Wang et al., 2016; Wu et al., 2017; Zhang and Sun, 2017). The suitable disposal of these wastes has become a crucial problem due to their rapid increase in production. Since composting is environmental friendliness and economic viability, it has been recognized as a popular method for the disposal of organic solid wastes (Huang et al., 2006; Wei et al., 2007; Yang et al., 2019).

During composting, dissolved organic matter (DOM) is converted from particulate organic matter by microorganisms (He et al., 2019; Xiao et al., 2019a). Many studies have shown that DOM is a heterogeneous mixture, including aliphatic, hydroxyl, carboxyl, carbonyl, and ester functional groups (Guo et al., 2019; Xiao et al., 2019a). Thus, when composting product is applied to arable land as a fertilizer or conditioner, the DOM may promote significant changes of soil properties (Beiyuan et al., 2018). Specifically, DOM can complex with multiple metals such as copper, lead, and zinc to change the solubility, transport, and toxicity of these metals in soil (Guo et al., 2019). DOM is also considered as an effective additive for the remediation of organically contaminated soil (Yu et al., 2011). The presence of DOM can significantly influence the behaviors of polycyclic aromatic hydrocarbons (PAHs), and polychlorinated biphenyls (PCBs) in soil (Badea et al., 2014; Smith et al., 2011; Yu et al., 2011). However, due to the heterogeneous nature of DOM, there have been inconsistent reports of the reaction between the DOM with contaminants (Xu et al., 2019). For example, algal-derived DOM and soil-derived DOM exhibited significantly different patterns of Cu(II) binding, indicating source-dependent metal binding heterogeneities of DOM (Xu et al., 2018). Therefore, for better agricultural utilization of various composts, it is essential to study the characteristics of the DOM derived from them.

Many technologies, particularly spectroscopic methods, have been applied to study the composition of compost-derived DOM, including fluorescence excitation/emission matrix (EEM), Fourier transform infrared (FTIR), ultraviolet/visible (UV/vis), and nuclear magnetic resonance (NMR) spectra (El Fels et al., 2014; Guo et al., 2019; Huang et al., 2018; Kovacevic et al., 2018; Liu et al., 2020b; Xiao et al., 2019b). These methods can reveal some information about the DOM features, such as elemental composition, apparent molecular weight, and the relative abundance of chemical groups (Lv et al., 2016a). However, due to the limitations of the methods used, more deriving information on DOM at the molecular level remain unknown (Lv et al., 2016b).

Mass spectrometry can also be used to investigate the structural characteristics of DOM. Recently, the development of a novel mass spectrometry analytical method, electrospray ionization coupled with Fourier transform ion cyclotron resonance mass spectrometry (ESI FT-ICR MS), has facilitated the more detailed analysis of DOM molecular composition (Kellerman et al., 2014). EST FT-ICR MS can measure the ion mass-to-charge ratio (m/z) based on the ion cyclotron frequency for a given magnetic field (Wang et al., 2018b). This method allows the sensitive detection of ionized organic compounds and classification of thousands of molecular formulas into major categories at the molecular level, such as CHO (containing only C, H, and O), CHON (containing C, H, O, and N), CHOS (containing C, H, O, and S), and CHONS (containing C, H, O, N, and S) (Chen et al., 2018). Many previous works have confirmed the use of ESI FT-ICR MS as an excellent technique to characterize DOM molecular compositions in atmospheric aerosols (Schmitt-Kopplin et al., 2010), rivers (Gonsior et al., 2016), leachate concentrates (Yuan et al., 2017), terrestrial soils (Chen et al., 2018), and hyperthermophilic composts of sewage sludge (Yu et al., 2019b). However, to the best of our knowledge, no study has utilized ESI FT-ICR MS to investigate the molecular characteristics of DOM derived from different source composts.

The goals of this study were to: (1) characterize the DOM molecular compositions of kitchen waste compost (KWC), green waste compost (GWC), manure waste compost (MWC), and sewage sludge compost (SSC) using ESI FT-ICR MS; (2) determine the similarities and differences of the source-dependent DOM molecular formulas; and (3) provide insights into the potential activities of various source composts during agricultural utilization.

1. Materials and methods

1.1. *Compost samples collection and DOM extraction*

Four compost samples (KWC, GWC, MWC, and SSC) were collected from full-scale composting plants, respectively located in Dongguan, Foshan, Baoding, and Zhengzhou of China, which respectively utilize kitchen waste, green waste, manure waste, and sewage sludge as the major composting raw materials. The composting took place in an in-vessel system and the loading capacity of each composting plants are more than 5 tons per day. Collected compost samples were determined to be mature, with a total duration of around 40 days. Two portions were taken from each sample. One was used to determine physicochemical properties, while the other was stored at 4 °C, before extracting the DOM. Details of the sample physical-chemical properties are listed in Appendix A **Table S1**.

DOM was extracted according to the method previously described by Yuan et al. (2012). Briefly, about 10 g of compost sample was mixed with 100 mL ultrapure water (purified with a Milli-Q purification system) and shaken in an oscillator at a rotational speed of 200 r/min for 24 hr. Then, the supernatant was centrifuged for 20 min at a rotational speed of 20,000 r/min and 4 °C. Finally, DOM was obtained when the supernatant was gravity-fed through a 0.45 μm filter. The amount of dissolved organic carbon (DOC) in each DOM sample was determined using a TOC instrument (TOC-L, Shimadzu, Japan). Subsequently, the four DOM samples were diluted to 20 mg/L DOC and acidified to pH 2 by the addition of high-purity hydrochloric acid for subsequent solid-phase extraction (SPE).

1.2. *Solid-phase extraction and ESI FT-ICR MS analysis*

SPE cartridges (Oasis HLB, USA) were used to purify the DOM samples. First, SPE cartridges were activated with 30 mL methanol (Chromasolv, Sigma Aldich) and then rinsed with 30 mL acidified ultrapure water (Milli-Q, pH 2, hydrochloric acid). Then, 10 mL DOM solutions were injected into the SPE cartridges. After allowing the DOM solutions to pass through the cartridges by gravity flow, the cartridges were again rinsed with 30 mL acidified ultrapure water (Milli-Q, pH 2, hydrochloric acid). The moisture in the cartridges was completely evaporated under a gentle N_2 stream. Finally, the samples were eluted from the SPE cartridges with 10 mL methanol (Chromasolv, Sigma Aldich). The purified methanolic DOM samples were obtained and stored at -18 °C prior to ESI FT-ICR MS analysis (Fan et al., 2016).

According to the previous method (Yu et al., 2019b), a SolariX XR FT-ICR MS (Bruker Daltonik GmbH, Germany)

equipped with a 9.4T refrigerated actively shielded superconducting magnet (Bruker Biospin, France) and a Paracell analyzer cell were employed to analyze the purified DOM samples. ESI ion mode (Bruker Daltonik GmbH, Germany) was used to ionize the DOM molecules, using an *m/z* range between 150 and 1200 and an ion accumulation time of 0.6 sec. The average mass resolution was >450,000 at *m/z* 319 with <0.3 ppm absolute mass error. Blank filters were similarly processed without sample application to detect possible contamination.

1.3. *Data visualization and interpretation*

Mathematically possible formulas for compounds in the four compost-derived DOM samples were calculated using custom software. The signal-to-noise ratio was above 10, and the mass tolerance was ±1 ppm. The double bound equivalent (DBE) indicated the degree of unsaturation (hydrogen deficiency) of a compound and was obtained according to the following equation: $DBE = (2c + 2 - h + n)/2$ (Hockaday et al., 2006); The modified aromaticity index (AI_{mod}), an empirical formulae of non aromatic (AI < 0.5), aromatic (AI > 0.5), and condensed aromatic (AI ≥ 0.67) compounds was calculated by the following equation: $AI_{mod} = (1+c-0.5o-s-0.5h)/(c-0.5o-s-n)$ (Koch and Dittmar, 2006). In the stated equations, the *c, h, o, n, s* represent the number of carbon, hydrogen, oxygen, nitrogen, and sulfur atoms in molecules, respectively. The processing details of other intensity-weighted averaged (w) values, such as the intensity-weighted averaged molecular weight (MW_w), H/C_w, O/C_w, N/C_w, S/C_w, DBE_w, and $AI_{mod,w}$, were previously described in the supporting information of Yuan et al. (2017) and Song et al. (2018), and are abbreviated as follows: $P_w = \frac{\sum(I_i \times P_i)}{\sum I_i}$, where P_w is the intensity weighted averaged (w) value of molecular weight, H/C, O/C, N/C, S/C, DBE, and AI_{mod}; I_i refers to the intensity for each individual molecular formula; and P_i represents the molecular weight, H/C, O/C, N/C, S/C, DBE, and AI_{mod} values for each individual molecular formula.

Van krevelen (VK) diagrams are widely used to show specific biochemical classes of DOM formulas based on different O/C and H/C ratios, including lipids, aliphatic/proteins, lignins/carboxylic-rich alicyclic molecules (CRAM), carbohydrates, unsaturated hydrocarbon, aromatic structures, and tannin (Yuan et al., 2017). VK analysis was classified as follows: lipids, H/C = 1.5–2.0, O/C = 0–0.3; aliphatic/proteins, H/C = 1.5–2.2, O/C = 0.3–0.67; lignins/CRAM, H/C = 0.7–1.5, O/C = 0.1–0.67; carbohydrates, H/C = 1.5–2.4, O/C = 0.67–1.2; unsaturated hydrocarbons, H/C = 0.7–1.5, O/C = 0–0.1; aromatic structures, H/C = 0.2–0.7, O/C = 0–0.67; and tannin, H/C = 0.6–1.5, O/C = 0.67–1.0.

2. Results and discussion

2.1. *General molecular characterizations of different compost-derived DOM*

Four compost-derived DOM samples were prepared for analysis. Appendix A **Fig. S1** shows the ESI FT-ICR mass spectra of the four samples. Thousands of peaks were observed between *m/z* 150 and 800 for each sample, and the vast majority of peaks were distributed within the *m/z* range of 200–600, similar to the results of previous DOM studies (Cao et al., 2015; Zhang et al., 2012). The mass spectra contours of the four DOM samples differed from each other in *m/z* values and intensities. According to the peak abundances, more than seven thousand molecular formulas were detected in each sample (Table 1). Those molecular formulas were classified into four major subcategories of CHO, CHON, CHOS, and CHONS based on their C, H, O, N, S compositions. Fig. 1 shows the VK diagram of the four major subcategories, their respective contributions, and biochemical classes for the four DOM samples. The percentages of CHON subcategory (35.8%-47.4%) and CHO subcategory (30.6%-40.9%), respectively represented the highest and the second highest fractions in KWC, MWC, and SSC DOM samples, while the percentage of CHO subcategory (68.4%) was the highest fraction and the percentage of CHON subcategory (26.4%) was the second highest fraction in GWC DOM sample (Fig. 1**b**). These results indicate larger proportions of nitrogen-containing (N-containing) species in KWC, MWC, and SSC DOM compared to the amount in GWC DOM. This difference may be explained based on the different composting raw materials used to generate these compost samples, because kitchen waste, manure waste, and sewage sludge generally have a lower C/N than green waste (Duan et al., 2019; González et al., 2019b; Yu et al., 2019a; Zhang et al., 2016). In addition, categories containing sulfur compounds (CHOS and CHONS) were 33.6% in SSC DOM, which accounted for the largest proportion among the four DOM samples. This was followed by MWC (22.9%), KWC (11.7%), and GWC (5.3%). Since odorous substances produced during composting mainly contain ammonia and hydrogen sulfide compounds (González et al., 2019a), it is highly important to control the odor for composting plants that use kitchen waste, manure waste, and sewage sludge as raw materials. Furthermore, since compost products are ultimately attributed to agricultural utilization, their nitrogen and sulfur contents may be tightly related to the soil nitrogen and sulfur cycles.

As shown in Fig. 1**a**, the VK diagram of DOM samples was divided into seven regions including lipids, aliphatic/proteins, carbohydrates, unsaturated hydrocarbons, lignins/CRAM, aromatic structures, and tannin. The percentages of the seven compounds are described in Fig. 1**c**. The lignins/CRAM structures were the most prevalent compounds in all DOM samples, accounting for 66.5%, 63.1%, 56.7%, and 51.6% of the KWC, GWC, SSC, and MWC DOM, respectively. In many natural DOM, such as material from rivers, terrestrial soils, and marine settings, the lignins/CRAM structures are always present at the highest levels and are typically the most stable compounds (Chen et al., 2018). The various DOM samples derived from composts may be an important source of stable soil organic carbon, which could contribute to the sequestration and storage of global organic carbon (Cooper et al., 2020). As shown in Fig. 1**c**, there were significantly higher proportions of aliphatic/protein structures in MWC DOM (25.1%) and SSC DOM (23.1%) compared to those in KWC DOM (15.3%) and GWC DOM (10.5%). This may be attributed to the presence of numerous N-containing compounds included in manure waste and sewage sludge. Protein structures are labile and continuously decomposed by microorganisms (Tuomela et al., 2000), and may eventually be transformed into humic substances.

The intensity-weighted averaged values for the molecular compositions of the four DOM samples were determined and are presented in Table 1. A total of 363, 385, 359, and 349 Da MW_w were observed in the KWC, GWC, MWC, and SSC DOM samples, respectively. Compared with the results from other works (Gonsior et al., 2016; Song et al., 2018), a source-dependent MW_w heterogeneity was observed in this study. The H/C_w, DBE_w, and $AI_{mod,w}$ values were previously related to unsaturated and aromatic components (Yuan et al., 2017). Compared to the KWC DOM (H/C_w = 1.28, DBE_w = 7.75, and $AI_{mod,w}$ = 0.26), MWC DOM (H/C_w = 1.34, DBE_w = 7.00, and $AI_{mod,w}$ = 0.24), and SSC DOM (H/C_w = 1.34, DBE_w = 6.53, and $AI_{mod,w}$ = 0.22), the GWC DOM (H/C_w = 1.15, DBE_w = 8.82, and $AI_{mod,w}$ =0.26) exhibited a lower H/C_w and higher DBE_w

Table 1 – Number of formulas and intensity weighted averaged (w) values for molecular composition of the four DOM samples.

Samples	Number of formulas	MW_w	H/C_w	O/C_w	N/C_w	S/C_w	DBE_w	$AI_{mod,w}$
KWC	7966	363	1.28	0.46	0.05	0.009	7.75	0.26
GWC	7947	385	1.15	0.51	0.02	0.004	8.82	0.26
MWC	7568	359	1.34	0.47	0.05	0.018	7.00	0.24
SSC	8324	349	1.34	0.50	0.04	0.028	6.53	0.22

KWC: kitchen waste compost; GWC: green waste compost; MWC: manure waste compost; SSC: sewage sludge compost (SSC).

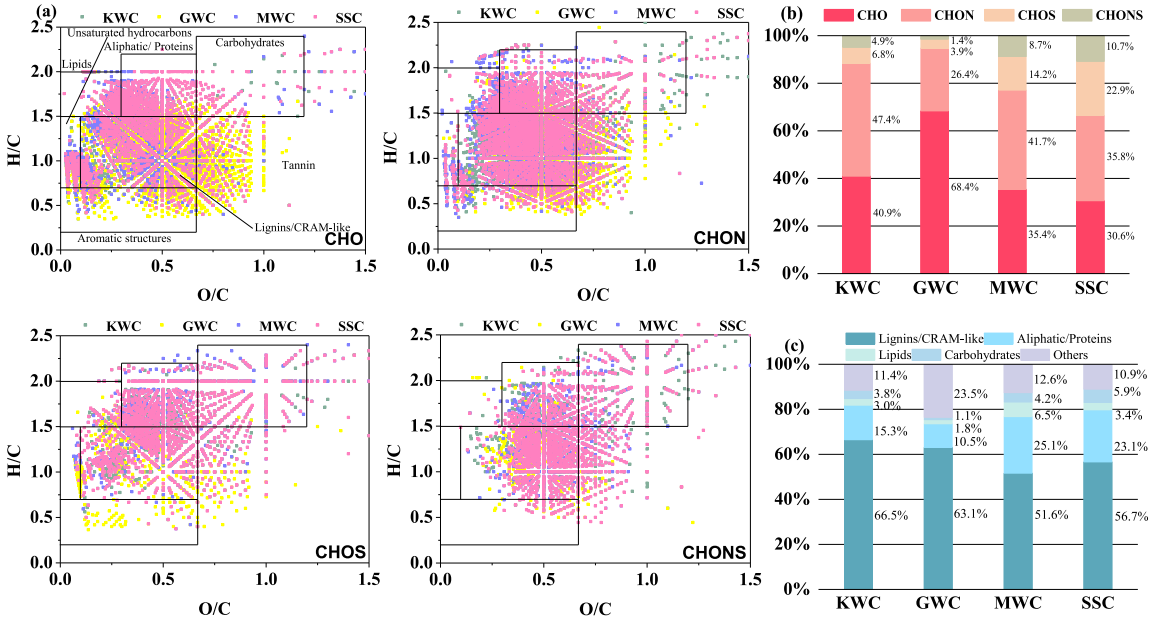

Fig. 1 – Comparison of DOM compositions in KWC, GWC, MWC and SSC samples. Dot diagrams (a) show the Van Krevelen diagram of the major subcategories (CHO, CHON, CHOS, CHONS) of the four samples. The composition domains separated by the black lines are the molecular formulae similar to lipids, aliphatic/proteins, carbohydrates, unsaturated hydrocarbons, lignins/CRAM-like, aromatic structures and tannin. Bar diagram (b) shows the contribution of the major subcategories (CHO, CHON, CHOS, CHONS). Bar diagram (c) shows the contribution of the major biochemical classes recognized in the Van Krevelen diagrams.

and $AI_{mod,w}$ values, suggesting that GWC DOM contained the most unsaturated and aromatic compounds. The O/C_w values of the four DOM samples exhibited the following trend: GWC>SSC>MWC>KWC. A higher O/C_w value indicates a higher degree of oxidation in DOM compounds (Yuan et al., 2017), suggesting the GWC DOM may have more oxidized compounds.

2.2. *CHO, CHON, CHOS, and CHONS compounds of DOM from different composts*

2.2.1. *CHO compounds*

As shown in Appendix A **Table S2**, a total of 2178, 3653, 2157, and 2054 molecular formulas could be assigned to CHO compounds in the KWC, GWC, MWC, and SSC DOM respectively. GWC DOM accounted for the highest fraction of the overall CHO compounds. A total of 338, 349, 357, and 379 Da MW_w were observed in SSC, KWC, MWC, and GWC DOM respectively. Compared with the MW_w of CHON, CHOS, and CHONS compounds, the MW_w of CHO compounds were much lower.

As the oxidation degree and unsaturation level of DOM compounds play a critical role in their adsorption behaviors and binding characteristics to contaminants (He et al., 2019; Wang et al., 2018a), the number of oxygens in the O_x class and the DBE_w of the CHO compounds was evaluated (Fig. 2). In general, oxygen atoms between 6 and 12 in the KWC and SSC DOM were well fitted by linear regression with DBE_w values, with coefficient of determination (R^2) values of 0.971 and 0.962, respectively. The number of oxygen atoms in the GWC DOM (6–19) and MWC DOM (6–16) were also well fitted by linear regression with DBE_w values, with R^2 values of 0.991 and 0.977, respectively. As shown by the dot diagram in Fig 2, outside of the ranges described above, there was no significant correlation between oxygen atoms and DBE_w.

The slopes and y-intercepts were also calculated. A slope of 0.5 was observed in the KWC DOM, indicating that approximately two oxygen atoms contribute to one DBE_w. Since a carboxyl group contains two oxygen atoms and one double bond, the CHO compounds in the KWC DOM may be carboxyl-rich, and their core molecular structures may not change significantly with only the subtraction or addition of multiple carboxyl groups. Since carboxyl groups in DOM were shown to exhibit a faster complex response to heavy metals, such as Cd

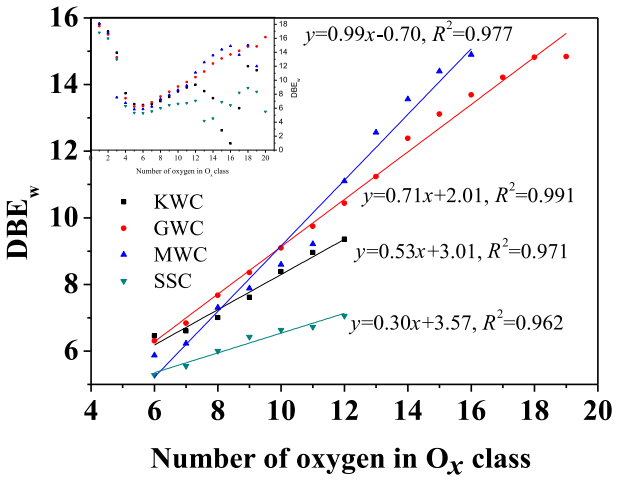

Fig. 2 – DBE_w is given as a function of the number of oxygen atoms obtained from CHO compounds of the four samples.

and Cu (Tang et al., 2019), KWC has potential for the efficient remediation of heavy metal-contaminated soil. The GWC and MWC DOM data exhibited slopes of 0.71 and 0.99, respectively, suggesting that the addition of two oxygen atoms resulted in approximate increases of 1.4 and 2.0 DBE_w. The larger DBE_w values can also be attributed to carboxyl groups, and other cyclic structures or unsaturated chemical bonds are also likely present. Alcohol and ether groups may also be present, but since they do not contain double bonds, there should be a much larger contribution of cyclic structures or unsaturated chemical bonds. Cyclic structures or unsaturated compounds exhibit higher adsorption capacity for organic pollutants (Wang et al., 2019), so they will affect the transfer and transformation of soil pollutants. In addition, a lower slope of 0.30 was observed in the SSC DOM, indicating that the addition of two oxygen atoms results in an increase of 0.6 DBE_w. This may reflect an increase of alcohol and ether groups and a decrease of carboxyl groups, cyclic structures, or unsaturated chemical bonds.

2.2.2. *CHON compounds*

As presented in Appendix A **Table S1**, the detected CHON compounds included 2979–3719 molecular formulas in the four samples. The MW_w values of CHON compounds were generally higher than those for CHO compounds. This indicated that an increase of N atoms resulted in a larger MW_w value. In addition, compared with the lower N/C_w value (0.073) determined for the GWC DOM, higher N/C_w values (0.093, 0.091, and 0.096) were observed in KWC, MWC, and SSC DOM. These observations once again demonstrated that GWC DOM contains compounds with lower levels of nitrogen.

Because nitrogenous compounds have vital effects on soil, further research was carried out on the CHON compounds subgroups according to the number of N and O atoms. As shown in Fig. 3, a total of 29 subgroups were identified including N_1O_x (N_1O_1- N_1O_{15}) and N_2O_x (N_2O_1- N_2O_{14}) compounds. According to a previous study (Song et al., 2018), some N_2O_x compounds may be dimers of N_1O_x compounds. For N_1O_x compounds, relatively high intensity contents were observed for N_1O_7-N_1O_9 (O/N = 7–9). This suggests that all the CHON subgroups present at relatively high abundance were rich in oxygen (O/N ≥ 7), and these compounds may also contain oxidized nitrogen functional groups such as $-NO_2$ and $-NO_3$ groups, as well as other oxygenated functional groups (Song et al., 2018). In contrast, for N_2O_x compounds, high intensity contents were observed for N_2O_6-N_2O_9 (O/N = 3–4.5), suggesting the potential presence of amide groups (Song et al., 2018). The N_2O_x compounds accounted for 16% of the CHON compounds in GWC DOM, which was significantly lower than the proportion of N_2O_x compounds in KWC DOM (40%), MWC DOM (35%), and SSC DOM (39%), suggesting that more N_1O_x compounds were present in GWC DOM.

As shown in Fig. 3, N_1O_8, N_1O_9, N_1O_9, and N_1O_7 class species were present at highest intensity in KWC, GWC, MWC, and SSC DOM; their DBE values versus carbon number are shown in Fig. 3. All of the highest intensity species contain more than 7 oxygen atoms. This may be related to the composting process in which organic substances are continuously oxidized, leading to an increase of carbonyl, carboxyl, and hydroxyl groups on the aromatic ring (Asses et al., 2018). We recognized several high-intensity formulas of the four class species, including $C_{18}H_{29}O_8N_1$, $C_{17}H_{25}O_8N_1$, and $C_{18}H_{27}O_8N_1$ in KWC DOM; $C_{14}H_{15}O_9N_1$, $C_{13}H_{13}O_9N_1$, and $C_{16}H_{17}O_9N_1$ in GWC DOM; $C_{33}H_{59}O_9N_1$, $C_{28}H_{47}O_9N_1$, and $C_{33}H_{57}O_9N_1$ in MWC DOM; and $C_{11}H_{15}O_7N_1$, $C_{11}H_{17}O_7N_1$, and $C_{12}H_{13}O_7N_1$ in SSC DOM. The C numbers of the high-intensity N_1O_8 species were 17–18 in KWC DOM, with DBE values 5–7. Compared with KWC DOM, lower C numbers (13–15, 10–12) and higher DBE values (8–9, 10–12) were observed in GWC DOM and SSC DOM, respectively. The C numbers of the high-intensity N_1O_9 species in MWC DOM were much higher than those of the other three samples. their C numbers were around 30 and their DBE values were maintained at 5–7. According to VK diagram, the high-intensity compounds of MWC DOM were almost classified into lipid, which may be related to some nitrogen-containing secondary metabolites in feed additives (Reddy et al., 2020),while those of the other three compost-derived DOM were almost classified into lignins/CRAM. According to the C, H, O, N numbers and DBE values of those compounds, it is not surprising that the aromatic and other heterocyclic aromatic compounds were dominant in those compounds, as well as oxygen-containing groups such as carbonyl, phenolic hydroxyl and carboxyl. According to the method of a previous study (Fang et al., 2017), one of the supposed structures of these most high-intensity compounds are listed in Fig. 3 except for MWC DOM, because their C numbers were much larger, and their structures were more complicated.

2.2.3. *CHOS compounds*

The number of molecular formulas for CHOS compounds ranged from 798–1692 (Appendix A **Table S2**). The lowest number (798) was found in the GWC DOM, which indicates a lower amount of sulfur-containing (S-containning) compounds. There were obviously lower numbers of CHOS molecular formulas than the numbers of CHO and CHON compounds. The MW_w values of the CHOS compounds were larger than those of CHO and CHON compounds, potentially due to the increase of sulfur atoms. The S/C_w values ranged from 0.069 to 0.081 in the four samples. The minimum S/C_w value of 0.069 was detected in GWC DOM, and the values were around 0.080 in the other three DOM samples. Similar to the results for the CHON compounds, the observations suggested that GWC DOM was also sulfur-deficient. This may be attributed to a lower N and S content in green waste (Bustamante et al., 2016).

According to the number of S and O atoms, a total of 24 subgroups were identified including O_xS_1 (O_3S_1-$O_{15}S_1$) and O_xS_2 (O_6S_2-$O_{16}S_2$) compounds. As shown in Fig. 4, the results clearly showed that most species were O_xS_1 compounds. The highest intensity species were O_3S_1, O_5S_1, O_8S_1, and O_5S_1 in KWC, GWC, MWC, and SSC DOM, respectively. For O_3S_1 compounds in KWC DOM, possible structures may include one C-O-S group and other alcoholic hydroxyl groups, such as

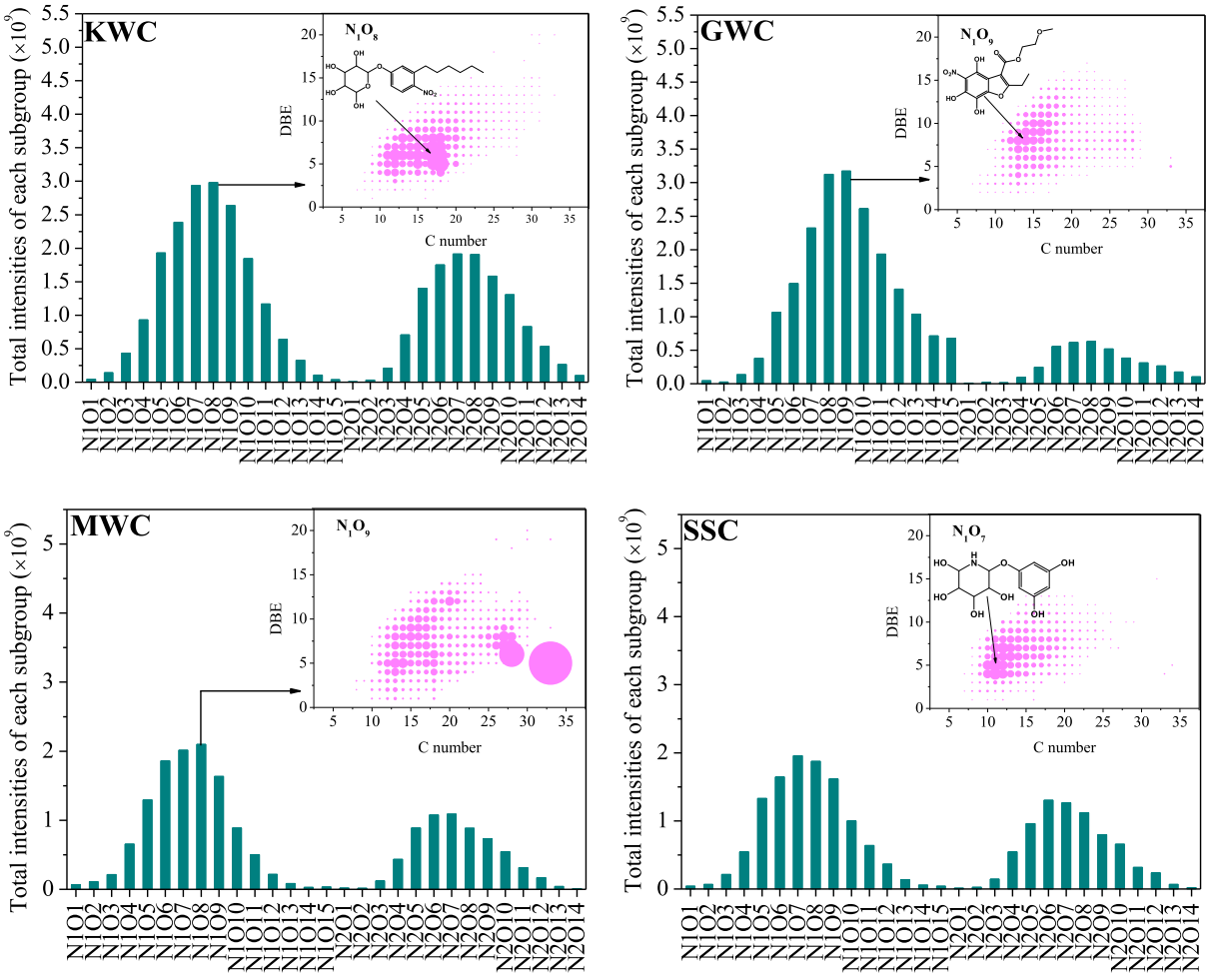

Fig. 3 – Classification of CHON compounds into different subgroups according to the number of N and O atoms in their molecules. The column is the sum of peak intensities in each subgroup. Attached figures exhibited the DBE values versus carbon number distribution of the highest intensity N_1O_8, N_1O_9, N_1O_9 and N_1O_7 class species in KWC, GWC, MWC and SSC respectively. The possible structures were proposed based on the molecular composition (the structures are just possible but not detected).

$C_{14}H_{28}O_3S_1$ and $C_{16}H_{32}O_3S_1$, both with 1 DBE value. In addition, we recognized the possible structure of the highest intensity compound ($C_{17}H_{28}O_3S$) in O_3S_1 species (Fig. 4), it may be humic-like substances which are widely produced during composting, and those compounds are stable and can resistant to biodegradation (Cui et al., 2019). According to a previous study (Lu et al., 2015), when O/S ≥4, organosulfates (R-O-SO_2-O-R', where R and R' can be alkane or aromatic hydrocarbon) may be present in CHOS compounds. Another report (Song et al., 2018) demonstrated that CHOS compounds such as $C_8H_{10}O_5S_1$ may include an alkylbenzene ring substituted with one sulfate and one hydroxyl group. Based on the molecular composition, the supposed structures of the highest intensity compounds in O_5S_1, O_8S_1, and O_5S_1 species in GWC, MWC, and SSC DOM are presented in Fig. 4. These compounds may include one alkylbenzene ring substituted with one sulfate and other hydroxyl or carbonyl groups. Additionally, the O_xS_2 species in CHOS compounds may contain both sulfinate and sulfonate groups (Fang et al., 2019).

2.2.4. *CHONS compounds*

As shown in Appendix A **Table S2**, 1074, 437, 1148, and 1599 CHONS compounds were detected in KWC, GWC, MWC, and SSC DOM, respectively. The CHONS compounds in GWC DOM (437) were significantly less than the other three samples. Compared with CHO, CHON, and CHOS compounds, CHONS compounds have the least molecular formulas and the highest MW_w values. The presence of N and S atoms increases the MW_w values. The $AI_{mod,w}$ values were 0.137, 0.306, 0.192, and 0.199 in KWC, GWC, MWC, and SSC DOM, respectively. Since the $AI_{mod,w}$ is a criterion of the compounds aromaticity, suggesting that S-containing compounds may contain fewer aromatic structures than CHO and CHON compounds.

As shown in Fig. 5, according to the number of N, O, and S atoms, the CHONS compounds included a wide variety of class species. $N_1O_4S_1$-$N_1O_{12}S_1$ compounds were most abundant in all samples. It was obvious that the total intensities of $N_1O_4S_1$-$N_1O_{12}S_1$ compounds in MWC DOM and SSC DOM were higher than those in KWC DOM and GWC DOM. There were also considerable amounts of $N_2O_6S_1$-$N_2O_{11}S_1$ in KWC, GWC, and SSC DOM. In all samples, there were more compounds contain-

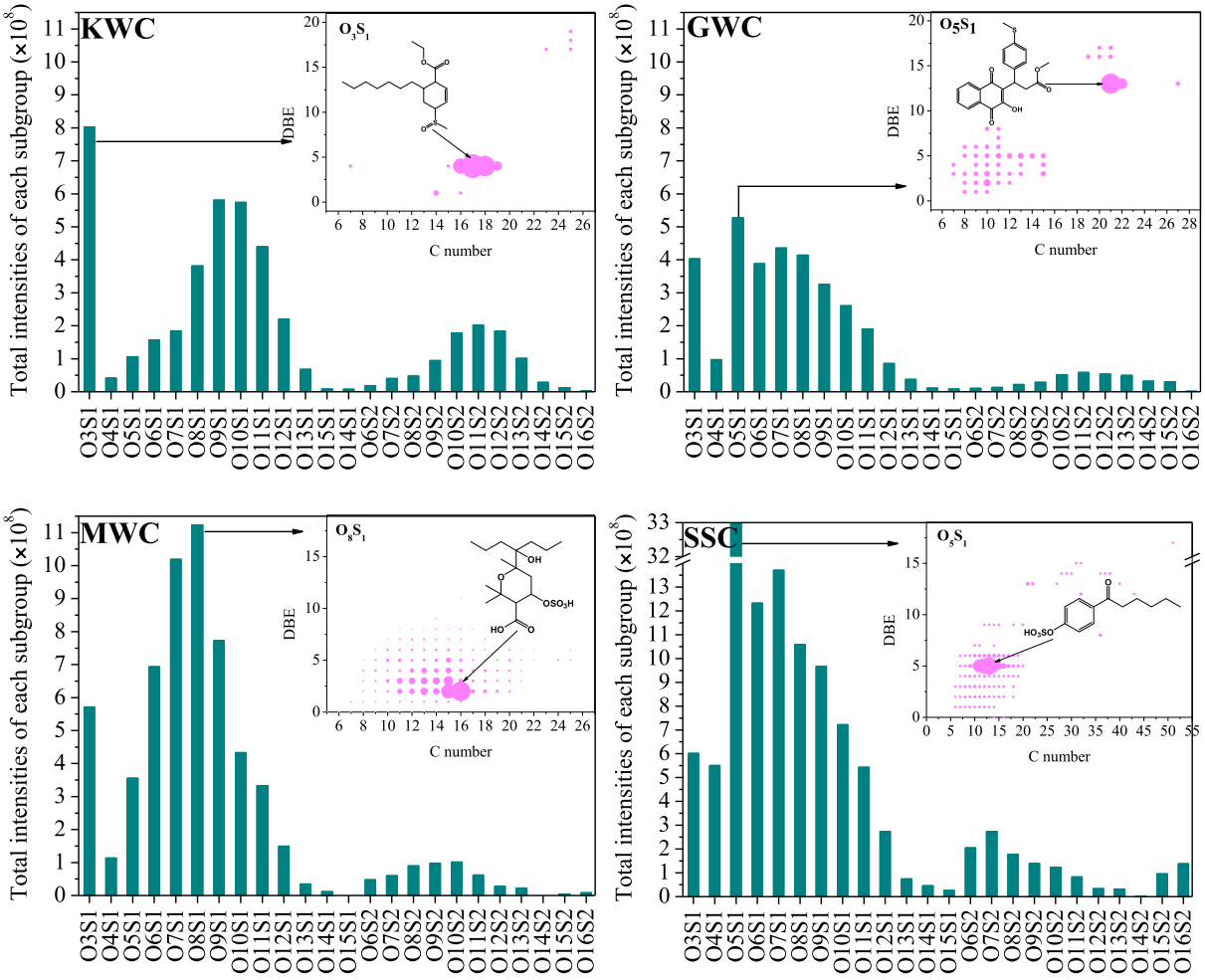

Fig. 4 – Classification of CHOS compounds into different subgroups according to the number of S and O atoms in their molecules. The column is the sum of peak intensities in each subgroup. Attached figures exhibited the DBE values versus carbon number distribution of the highest intensity O_3S_1, O_5S_1, O_8S_1 and O_5S_1 class species in KWC, GWC, MWC and SSC respectively. The possible structures were proposed based on the molecular composition (the structures are just possible but not detected).

ing one sulfur atom and one nitrogen atom than other compounds, such as compounds containing one sulfur atom and two nitrogen atoms or containing two sulfur atoms and one nitrogen atom. $N_1O_{10}S_1$, $N_1O_7S_1$, $N_1O_7S_1$, and $N_1O_8S_1$ were the most abundant species detected in KWC, GWC, MWC, and SSC DOM samples, respectively. With a relatively high number of O atoms (>7), this result may imply that some nitrogen atoms in CHONS compounds may exist as $–NO_2$ groups, and some S atoms may exist as sulfonate groups, as well as sulfonamides or other metabolites (Yuan et al., 2017).

Table 2 – Number of formulas and intensity weighted averaged (w) values for similar and unique molecular composition of the samples.

	Samples	Number of formulas	MW_w	H/C_w	O/C_w	N/C_w	S/C_w	DBE_w	$AI_{mod,w}$
Similar	Four DOM samples	3062	337	1.28	0.45	0.04	0.001	7.24	0.28
Unique	KWC	1486	524	1.37	0.44	0.05	0.030	9.83	0.24
	GWC	2338	532	1.01	0.56	0.01	0.006	12.80	0.36
	MWC	850	476	1.48	0.40	0.04	0.032	8.17	0.26
	SSC	1478	427	1.47	0.48	0.03	0.065	6.56	0.18

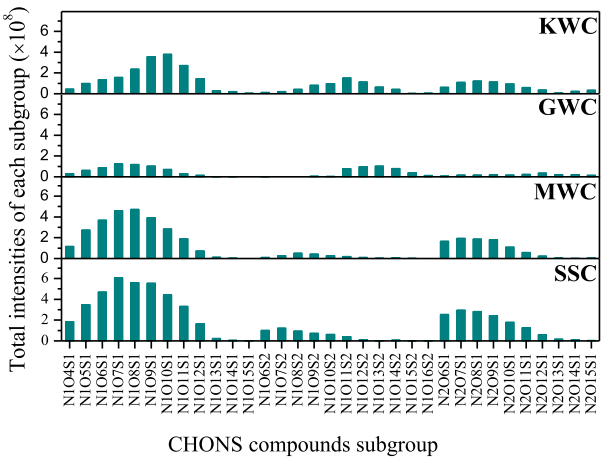

Fig. 5 – Classification of CHOS compounds into different subgroups according to the number of N, S and O atoms in their molecules. The high column is the sum of peak intensities in each subgroup.

2.3. *Similarities and differences of DOM derived from different composts*

Venn diagrams are widely used to represent overlap of molecular formulas (Qiu et al., 2020). In our study, the similarities of the four DOM samples were represented by the ubiquitous molecular formulas which were shown as overlapping molecular formulas in Fig. 6a and accounted for 22.8% of the total compounds. The differences of the four DOM samples were represented by the unique molecular formulas which did not overlap with the formulas of compounds in the other three samples (Fig. 6a), with 17.4%, 11.1%, 10.7%, and 6.3% for GWC, KWC, SSC, and MWC DOM respectively. To better understand the similarities and differences of the four samples, the shared and unique compounds were investigated. As shown in Table 2, 3062 molecular formulas were common to all four samples, a number that is obviously higher than the number of unique molecular formulas of KWC DOM (1486), GWC DOM (2338), MWC DOM (850) and SSC DOM (1478). Compared with the MW_w (427–532 Da) of unique molecular compositions, a lower MW_w (337 Da) was observed for the common molecular compositions. Since DOM with low molecular weight are highly labile and easily used by microorganisms (Brailsford et al., 2017), these widespread compounds may be more preferentially converted in soil. The compounds present in all four DOM samples would have similar effects on soil properties, but the unique compounds may result in different effects for agricultural applications. The N/C_w and S/C_w values of unique molecular compositions were significantly different. The highest N/C_w value (0.05) was found in KWC DOM, which might be attributable to a greater percentage of the sequestration N formed during kitchen waste composting (Liu et al., 2020a). This result suggested that KWC DOM has a more stable supply of organic nitrogen to soil than the other three DOM. The highest S/C_w value (0.065) of unique molecular compositions was observed in SSC DOM, Since organic S-containing compounds can be converted into more labile S compounds including SO_4^{2-} in the presence of microbes (Luo et al., 2014). Long-term application of SSC may cause soil acidification. The S/C_w values in unique formulas were 0.030, 0.006, 0.032, and 0.065, which were much higher than that 0.001 for the common compounds. This suggested that the presence of sulfur-containing compounds explained the differences of the four samples. The H/C_w, DBE_w, $AI_{mod,w}$, and O/C_w values between similar and unique molecular compositions did not exhibit obvious patterns, but interestingly, the lowest H/C_w and the highest DBE_w, $AI_{mod,w}$, and O/C_w were observed in unique compositions of GWC DOM. This further indicated that the unique compounds in GWC DOM were less saturated, more aromatic, and oxidized.

To further compare the similarities and differences of the four samples, a comprehensive description of C numbers, DBEs, peak intensities, and O atoms of the ubiquitous and unique molecular compounds is presented in Fig. 6b and Fig. 6c. The C numbers of ubiquitous molecular formulas mainly ranged from 10 to 30, and the DBE values were distributed in a range of 0–20. The high-intensity compounds of ubiquitous compositions were mainly concentrated in two regions: C numbers (10–20) with DBE values (4–8) and C numbers (25–30) with DBE values (16–18). Both sets of compounds had relatively lower amounts of oxygen. Moreover, C numbers with a range of 0–40 were observed in all unique compositions. A wide range of DBEs (0–20) was also detected in all unique compositions. In addition, a clear trend toward increasing DBE values with increasing carbon numbers was also found in all unique compositions. The most represented compounds with unique compositions were mostly compounds with relatively higher oxygen levels, and their distributions showed significant variability, such as the majority of compounds in GWC DOM had C numbers of 10–30 and DBE values of 5–15, but the majority of compounds in SSC DOM had C numbers of 10–20 and DBE values of 4–8. These observations suggested that DOM derived from different compost sources contained distinct compounds.

3. Conclusions

This study comprehensively characterized the molecular compositions of DOM from KWC, GWC, MWC and SSC and determined the similarities and differences in the DOM samples based on the detection of common and unique molecular formulas. The source heterogeneity of DOM molecular compositions could influence the behaviors of various composts during agricultural utilization. Here, GWC DOM were deficient in nitrogen- and sulfur-containing compounds, suggesting that they may not be ideal for treatment of nitrogen-deficient soil. KWC, MWC and SSC DOM might be better choices, but the higher sulfur content of these composts especially in SSC DOM is worth consideration. The highest percentage of lignin compounds in all DOM samples suggested that composts may be a source of stable organic carbon for soil, and could contribute to the sequestration and storage of global organic carbon. The recognition of possible structures of CHO, CHON, CHOS and CHONS subcategories of the four DOM samples could help us to better understand the potential role of different composts for soil remediation. Furthermore, the compounds present in all four samples exhibited relatively lower MW_w and oxygen contents, suggesting these compounds may be more preferentially converted in soil. While, the unique compositions in the four samples showed relatively higher MW_w and oxygen contents, mainly due to the presence of sulfur-containing compounds. Our work showed that ESI FT-ICR MS was very effective to achieve a better understanding of the molecular compositions of DOM derived from various composts. However, some questions still remain to be answered in the future. The potential changes of the molecular characteristics of DOM during the composting process should be further determined; the transformation of DOM derived from different composts in soil should be characterized at the

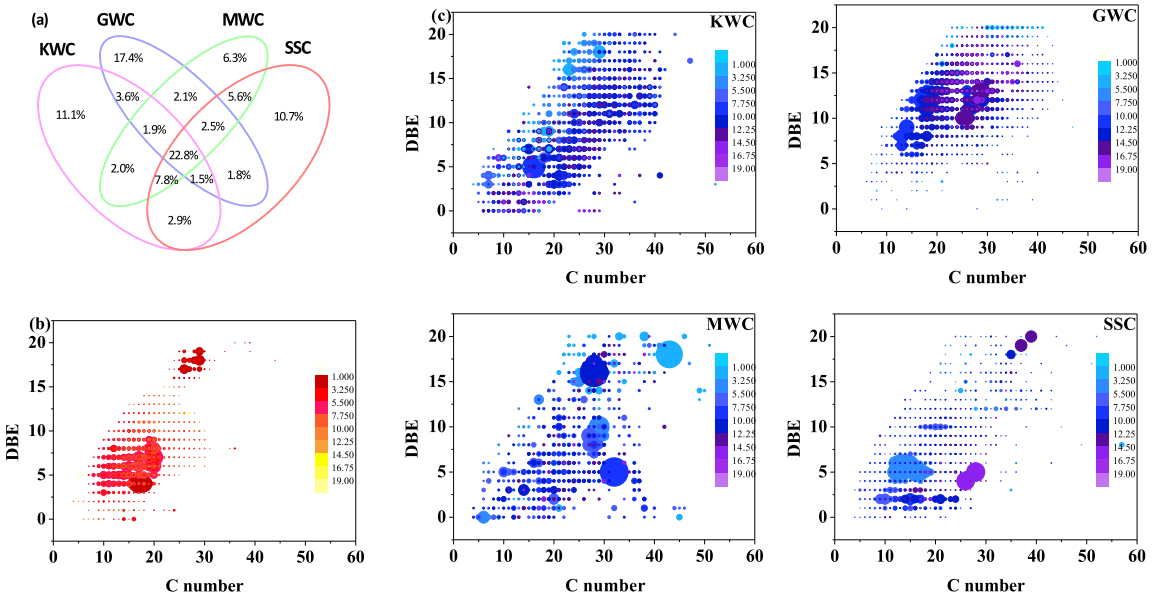

Fig. 6 – Venn diagram (a) shows the relative distributions of all molecular formulas present in the four samples. In Venn diagram, percentages in areas of overlap are percentages of molecular formulas that appear in both, three or all four of those samples. Percentages in areas with no overlap are unique to that individual sample. Dot diagram (b) shows the C number and DBEs of the overlap molecular compounds of the four samples. Dot diagram (c) shows the C number and DBEs of the unique molecular compounds of the four samples. The circle size and the color bar represent the peak intensities and the number of O atoms respectively.

molecular level; additionally, the detailed mechanisms of how DOM interacts with soil contaminants should be investigated.

Acknowledgements

This work was supported by the GDAS' Project of Science and Technology Development (No. 2019GDASYL-0501005); the Natural Science Foundation of Guangdong Province (No. 2018A030310084); a development project of Ronggui's strategic emerging industries (Ronggui Jingfa [2019] Reference No.19); and the Program of Guangdong Provincial Key Laboratory of New and Renewable Energy Research and Development, China (No. y809jm1001).

Appendix A. Supplementary data

Supplementary material associated with this article can be found, in the online version, at doi:10.1016/j.jes.2020.06.011.

REFERENCES

Asses, N., Farhat, A., Cherif, S., Hamdi, M., Bouallagui, H., 2018. Comparative study of sewage sludge co-composting with olive mill wastes or green residues: Process monitoring and agriculture value of the resulting composts. Process Saf. Environ. Protect. 114, 25–35.

Badea, S.L., Mustafa, M., Lundstedt, S., Tysklind, M., 2014. Leachability and desorption of PCBs from soil and their dependency on pH and dissolved organic matter. Sci. Total Environ. 499, 220–227.

Beiyuan, J., Tsang, D.C.W., Bolan, N.S., Baek, K., Ok, Y.S., Li, X.D., 2018. Interactions of food waste compost with metals and metal-chelant complexes during soil remediation. J. Clean Prod. 192, 199–206.

Brailsford, F.L., Glanville, H.C., Marshall, M.R., Golyshin, P.N., Johnes, P.J., Yates, C.A., et al., 2017. . Microbial use of low molecular weight DOM in filtered and unfiltered freshwater: Role of ultra-small microorganisms and implications for water quality monitoring. Sci. Total Environ. 598, 377–384.

Bustamante, M.A., Ceglie, F.G., Aly, A., Mihreteab, H.T., Ciaccia, C., Tittarelli, F., 2016. Phosphorus availability from rock phosphate: Combined effect of green waste composting and sulfur addition. J. Environ. Manage. 182, 557–563.

Cao, D., Huang, H.G., Hu, M., Cui, L., Geng, F.L., Rao, Z.Y., et al., 2015. Comprehensive characterization of natural organic matter by MALDI- and ESI-Fourier transform ion cyclotron resonance mass spectrometry. Anal. Chim. Acta 866, 48–58.

Chen, H.M., Yang, Z.M., Chu, R.K., Tolic, N., Liang, L.Y., Graham, D.E., et al., 2018. . Molecular insights into arctic soil organic matter degradation under warming. Environ. Sci. Technol. 52 (8), 4555–4564.

Cooper, J., Greenberg, I., Ludwig, B., Hippich, L., Fischer, D., Glaser, B., et al., 2020. Effect of biochar and compost on soil properties and organic matter in aggregate size fractions under field conditions. Agric. Ecosyst. Environ. 295, 106882.

Cui, P., Liao, H.P., Bai, Y.D., Li, X., Zhao, Q., Chen, Z., et al., 2019. Hyperthermophilic composting reduces nitrogen loss via inhibiting ammonifiers and enhancing nitrogenous humic substance formation. Sci. Total Environ. 692, 98–106.

Duan, Y.M., Awasthi, S.K., Chen, H.Y., Liu, T., Zhang, Z.Q., Zhang, L.S., et al., 2019. Evaluating the impact of bamboo biochar on the fungal community succession during chicken manure composting. Bioresour. Technol. 272, 308–314.

El Fels, L., Zamama, M., El Asli, A., Hafidi, M., 2014. Assessment of biotransformation of organic matter during co-composting of sewage sludge-lignocelullosic waste by chemical, FTIR analyses, and phytotoxicity tests. Int. Biodeterior. Biodegrad. 87, 128–137.

Fan, X.J., Wei, S.Y., Zhu, M.B., Song, J.Z., Peng, P.A., 2016. Comprehensive characterization of humic-like substances in smoke PM2.5 emitted from the combustion of biomass materials and fossil fuels. Atmos. Chem. Phys. 16 (20), 13321–13340.

Fang, Z., He, C., Li, Y.Y., Chung, K.H., Xu, C.M., Shi, Q., 2017. Fractionation and characterization of dissolved organic matter (DOM) in refinery wastewater by revised phase retention and ion-exchange adsorption solid phase extraction followed by ESI FT-ICR MS. Talanta 162, 466–473.

Fang, Z., Li, L.J., Jiang, B., He, C., Li, Y.Y., Xu, C.M., et al., 2019. Molecular composition and transformation of dissolved organic matter (DOM) in coal gasification wastewater. Energy Fuels 33 (4), 3003–3011.

Gonsior, M., Valle, J., Schmitt-Kopplin, P., Hertkorn, N., Bastviken, D., Luek, J., et al., 2016. Chemodiversity of dissolved organic matter in the Amazon Basin. Biogeosciences 13, 1–21.

González, D., Colón, J., Gabriel, D., Sánchez, A., 2019a. The effect of the composting time on the gaseous emissions and the compost stability in a full-scale sewage sludge composting plant. Sci. Total Environ. 654, 311–323.

González, D., Colón, J., Sánchez, A., Gabriel, D., 2019b. A systematic study on the VOCs characterization and odour emissions in a full-scale sewage sludge composting plant. J. Hazard. Mater. 373, 733–740.
Guo, X.J., He, X.S., Li, C.W., Li, N.X., 2019. The binding properties of copper and lead onto compost-derived DOM using Fourier-transform infrared, UV–vis and fluorescence spectra combined with two-dimensional correlation analysis. J. Hazard. Mater 365, 457–466.
He, X.S., Yang, C., You, S.H., Zhang, H., Xi, B.D., Yu, M.D., et al., 2019. Redox properties of compost-derived organic matter and their association with polarity and molecular weight. Sci. Total Environ. 665, 920–928.
Hockaday, W.C., Grannas, A.M., Kim, S., Hatcher, P.G., 2006. Direct molecular evidence for the degradation and mobility of black carbon in soils from ultrahigh-resolution mass spectral analysis of dissolved organic matter from a fire-impacted forest soil. Org. Geochem. 37 (4), 501–510.
Huang, G.F., Wu, Q.T., Wong, J.W.C., Nagar, B.B., 2006. Transformation of organic matter during co-composting of pig manure with sawdust. Bioresour. Technol. 97 (15), 1834–1842.
Huang, M., Li, Z.W., Huang, B., Luo, N.L., Zhang, Q., Zhai, X.Q., et al., 2018. Investigating binding characteristics of cadmium and copper to DOM derived from compost and rice straw using EEM-PARAFAC combined with two-dimensional FTIR correlation analyses. J. Hazard. Mater. 344, 539–548.
Kellerman, A., Dittmar, T., Kothawala, D., Tranvik, L., 2014. Chemodiversity of dissolved organic matter in lakes driven by climate and hydrology. Nat. Commun. 5, 3804.
Koch, B., Dittmar, T., 2006. From mass to structure: An aromaticity index for high-resolution mass data of natural organic matter. Rapid Commun. Mass Spectrom. 20, 926–932.
Kovacevic, V., Simpson, A.J., Simpson, M.J., 2018. Evaluation of Daphnia magna metabolic responses to organic contaminant exposure with and without dissolved organic matter using 1H nuclear magnetic resonance (NMR)-based metabolomics. Ecotox. Environ. Safe. 164, 189–200.
Liu, S.S., He, Z.Q., Tang, Z., Liu, L.Z., Hou, J.W., Li, T.T., et al., 2020a. Linking the molecular composition of autochthonous dissolved organic matter to source identification for freshwater lake ecosystems by combination of optical spectroscopy and FT-ICR-MS analysis. Sci. Total Environ. 703, 134764.
Liu, W., Huo, R., Xu, J.X., Liang, S.X., Li, J.J., Zhao, T.K., et al., 2017. Effects of biochar on nitrogen transformation and heavy metals in sludge composting. Bioresour. Technol. 235, 43–49.
Liu, X.M., Hou, Y., Li, Z., Yu, Z., Tang, J., Wang, Y.Q., et al., 2020b. Hyperthermophilic composting of sewage sludge accelerates humic acid formation: Elemental and spectroscopic evidence. Waste Manage 103, 342–351.
Lu, Y.H., Li, X.P., Mesfioui, R., Bauer, J.E., Chambers, R.M., Canuel, E.A., et al., 2015. Use of ESI-FTICR-MS to characterize dissolved organic matter in headwater streams draining forest-dominated and pasture-dominated satersheds. PLoS ONE 10 (12), e0145639.
Luo, L., Xu, C., Ma, Y.B., Zheng, L., Liu, L.J., Lv, J.T., et al., 2014. Sulfur speciation in an arable soil as affected by sample pretreatments and sewage sludge application. Soil Sci. Soc. Am. J. 78 (5), 1615–1623.
Lv, J.T., Zhang, S.Z., Luo, L., Cao, D., 2016a. Solid-phase extraction-stepwise elution (SPE-SE) procedure for isolation of dissolved organic matter prior to ESI-FT-ICR-MS analysis. Anal. Chim. Acta 948, 55–61.
Lv, J.T., Zhang, S.Z., Wang, S.S., Luo, L., Cao, D., Christie, P., 2016b. Molecular-scale investigation with ESI-FT-ICR-MS on fractionation of dissolved organic matter induced by adsorption on iron oxyhydroxides. Environ. Sci. Technol. 50 (5), 2328–2336.
Qiu, J.J., Lu, F., Zhang, H., Huang, Y.L., Shao, L.M., He, P.J., 2020. Persistence of native and bio-derived molecules of dissolved organic matters during simultaneous denitrification and methanogenesis for fresh waste leachate. Water Res 175, 115705.
Reddy, P.R.K., Elghandour, M.M.M.Y., Salem, A.Z.M., Yasaswini, D., Reddy, P.P.R., Reddy, A.N., et al., 2020. Plant secondary metabolites as feed additives in calves for antimicrobial stewardship. Anim. Feed Sci. Technol. 264, 114469.
Schmitt-Kopplin, P., Gelencsér, A., Dabek-Zlotorzynska, E., Kiss, G., Hertkorn, N., Harir, M., et al., 2010. Analysis of the unresolved organic fraction in atmospheric aerosols with ultrahigh-resolution mass spectrometry and nuclear magnetic resonance spectroscopy: Organosulfates as photochemical smog constituents. Anal. Chem. 82 (19), 8017–8026.
Smith, K.E.C., Thullner, M., Wick, L.Y., Harms, H., 2011. Dissolved organic carbon enhances the mass transfer of hydrophobic organic compounds from nonaqueous phase liquids (NAPLs) into the aqueous phase. Environ. Sci. Technol. 45 (20), 8741–8747.
Song, J.Z., Li, M.J., Jiang, B., Wei, S.Y., Fan, X.J., Peng, P.A., 2018. Molecular characterization of water-soluble humic like substances in smoke particles emitted from combustion of biomass materials and coal using Ultrahigh-Resolution Electrospray Ionization Fourier Transform Ion Cyclotron Resonance Mass Spectrometry. Environ. Sci. Technol. 52 (5), 2575–2585.
Tang, J., Zhuang, L., Yu, Z., Liu, X.M., Wang, Y.Q., Wen, P., et al., 2019. Insight into complexation of Cu(II) to hyperthermophilic compost-derived humic acids by EEM-PARAFAC combined with heterospectral two dimensional correlation analyses. Sci. Total Environ. 656, 29–38.
Tuomela, M., Vikman, M., Hatakka, A., Itävaara, M., 2000. Biodegradation of lignin in a compost environment: a review. Bioresour. Technol. 72 (2), 169–183.
Wang, B., Zeng, D., Chen, Y.W., Belzile, N., Bai, Y.C., Zhu, J.P., et al., 2019. Adsorption behaviors of phenanthrene and bisphenol A in purple paddy soils amended with straw-derived DOM in the West Sichuan Plain of China. Ecotox. Environ. Safe. 169, 737–746.
Wang, Q., Awasthi, M.K., Zhao, J.C., Ren, X.N., Wang, M.J., Li, R.H., et al., 2018a. Utilization of medical stone to improve the composition and quality of dissolved organic matter in composted pig manure. J. Clean Prod. 197, 472–478.
Wang, X., Wang, J., Li, K.Y., Zhang, H.F., Yang, M., 2018b. Molecular characterization of effluent organic matter in secondary effluent and reclaimed water: Comparison to natural organic matter in source water. J. Environ. Sci. 63, 140–146.
Wang, X.J., Zhang, W.W., Gu, J., Gao, H., Qin, Q.J., 2016. Effects of different bulking agents on the maturity, enzymatic activity, and microbial community functional diversity of kitchen waste compost. Environ. Technol. 37 (20), 2555–2563.
Wei, Z.M., Xi, B.D., Zhao, Y., Wang, S.P., Liu, H.L., Jiang, Y.H., 2007. Effect of inoculating microbes in municipal solid waste composting on characteristics of humic acid. Chemosphere 68 (2), 368–374.
Wu, S.H., Shen, Z.Q., Yang, C.P., Zhou, Y.X., Li, X., Zeng, G.M., 2017. Effects of C/N ratio and bulking agent on speciation of Zn and Cu and enzymatic activity during pig manure composting. Int. Biodeterior. Biodegrad. 119, 429–436.
Xiao, X., Xi, B.D., He, X.S., Zhang, H., Li, D., Zhao, X.Y., et al., 2019a. Hydrophobicity-dependent electron transfer capacities of dissolved organic matter derived from chicken manure compost. Chemosphere 222, 757–765.
Xiao, X., Xi, B.D., He, X.S., Zhang, H., Li, Y.H., Pu, S., et al., 2019b. Redox properties and dechlorination capacities of landfill-derived humic-like acids. Environ. Pollut. 253, 488–496.
Xu, H.C., Guan, D.X., Zou, L., Lin, H., Guo, L.D., 2018. Contrasting effects of photochemical and microbial degradation on Cu(II) binding with fluorescent DOM from different origins. Environ. Pollut. 239, 205–214.
Xu, H.C., Zou, L., Guan, D.X., Li, W.T., Jiang, H.L., 2019. Molecular weight-dependent spectral and metal binding properties of sediment dissolved organic matter from different origins. Sci. Total Environ. 665, 828–835.
Yang, F., Li, Y., Han, Y.H., Qian, W.T., Li, G.X., Luo, W.H., 2019. Performance of mature compost to control gaseous emissions in kitchen waste composting. Sci. Total Environ. 657, 262–269.
Yu, H., Huang, G.H., An, C.J., Wei, J., 2011. Combined effects of DOM extracted from site soil/compost and biosurfactant on the sorption and desorption of PAHs in a soil-water system. J. Hazard. Mater. 190 (1), 883–890.
Yu, K.F., Li, S.Y., Sun, X.Y., Cai, L.L., Zhang, P.F., Kang, Y., et al., 2019a. . Application of seasonal freeze-thaw to pretreat raw material for accelerating green waste composting. J. Environ. Manage. 239, 96–102.
Yu, Z., Liu, X.M., Chen, C.Y., Liao, H.P., Chen, Z., Zhou, S.G., 2019b. Molecular insights into the transformation of dissolved organic matter during hyperthermophilic composting using ESI FT-ICR MS. Bioresour. Technol. 292, 122007.
Yuan, Y., Tao, Y., Zhou, S.G., Yuan, T., Lu, Q., He, J., 2012. Electron transfer capacity as a rapid and simple maturity index for compost. Bioresour. Technol. 116, 428–434.
Yuan, Z.W., He, C., Shi, Q., Xu, C.M., Li, Z.S., Wang, C.Z., et al., 2017. Molecular insights into the transformation of dissolved organic matter in landfill leachate concentrate during biodegradation and coagulation processes using ESI FT-ICR MS. Environ. Sci. Technol. 51 (14), 8110–8118.
Zhang, H.Y., Li, G.X., Gu, J., Wang, G.Q., Li, Y.Y., Zhang, D.F., 2016. Influence of aeration on volatile sulfur compounds (VSCs) and NH_3 emissions during aerobic composting of kitchen waste. Waste Manage. 58, 369–375.
Zhang, H.F., Zhang, Y.H., Shi, Q., Ren, S.Y., Yu, J.W., Ji, F., et al., 2012. Characterization of low molecular weight dissolved natural organic matter along the treatment trait of a waterworks using Fourier transform ion cyclotron resonance mass spectrometry. Water Res. 46 (16), 5197–5204.
Zhang, L., Sun, X.Y., 2017. Addition of seaweed and bentonite accelerates the two-stage composting of green waste. Bioresour. Technol. 243, 154–162.